

## FEDSM-ICNMM2010-30801

### LIQUID DEPOSITION AT MICRO AND NANOSCALE

Artur LUTFURAKHMANOV, Robert SAILER, Gregory LOKEN, Ananiy KOHUT,  
Yechun WANG, Andriy VORONOV, Douglas L. SCHULZ, Iskander S. AKHATOV

North Dakota State University, Fargo, ND, 58108, USA

#### ABSTRACT

Micro/Nanolithography is a creation of micro/nano features on the substrate. This paper proposes a new capillary-based lithography method that is non-invasive to substrate. The application of the pressure from one side of capillary causes the liquid meniscus to form at the capillary outlet. Touching the substrate with the meniscus only causes the liquid deposition on the substrate. The size of deposited liquid droplet is about 10% of inner diameter of the capillary. Glycerol was chosen as a trial liquid of deposition, because the rate of evaporation for glycerol is low in comparison with other liquids. The deposition of glycerol was done in micro-scale. Comparison of theoretical results with experimental data is shown and discussed.

**Keywords:** Micro-Capillary, Liquid Droplet, Surface Tension

#### 1. INTRODUCTION

The on-demand deposition of micro- and nanometer scale liquid droplets onto the substrate is an important task for many applications in microelectronics and biotechnology. The substantial efforts in designing and manufacturing novel dispensing devices have already enabled breakthroughs in these areas [1-3]. From physics of fluids perspective, there are two questions: (1) when a steady liquid bridge can be formed between dispensing tip and substrate? and (2) what happens with the liquid bridge when the tip moves up and away from the substrate causing bridge to break, leaving residual droplet on the substrate. Question (2) was addressed recently in Ref. [4] where dynamics of liquid bridge and subsequent droplet deposition was studied. It was experimentally shown that a wide range of droplet sizes results from the same capillary, depending strongly on the capillary retraction speed. In this paper, we present theoretical solution for the shape of the liquid

bridge that forms at the moment when the liquid meniscus protruding out of the capillary comes into contact with the substrate. We also demonstrate our theoretical and experimental studies on how this shape may change with the subsequent careful manipulation of the distance between capillary tip and the substrate.

#### 2. THEORY

The liquid bridge and the liquid between the hypothetical piston and the capillary edge marked on Fig. 1 as  $V_B$  and  $V_C$  respectively, can be considered as a closed system at constant pressure, temperature, and mass (volume). Radius of the capillary is small ( $Bo = \rho g r_c^2 / \gamma_{LV} \ll 1$ ) so that liquid pressure is uniform in the bridge.

The steady bridge forms when the work of external forces on the system's virtual displacement,  $\delta W_{ext}$  is equal to the variation of surface energy of the system,  $\delta E_\Sigma$ :

$$\delta W_{ext} = \delta E_\Sigma \quad (1)$$

$$\delta W_{ext} = -p dV_C - p_0 dV_B = (p - p_0) dV_B, \quad dV_C = -dV_B \quad (2)$$

$$\delta E_\Sigma = \gamma_{LV} \delta A_{LV} + (\gamma_{LS} - \gamma_{SV}) \delta A_{LS}, \quad (3)$$

Here  $p$  is pressure in the liquid bridge,  $p_0$  is pressure in a surrounding atmosphere,  $V_C$  is volume of the liquid between piston and capillary edge,  $V_B$  is volume of the liquid bridge (between capillary edge and the substrate),  $A_{LV}$  is area of the liquid bridge-vapor interface,  $A_{LS}$  is area of the liquid bridge-substrate interface, and  $\gamma_{LV}, \gamma_{LS}, \gamma_{SV}$  are energy of liquid-

vapor, liquid-substrate, and substrate-vapor interface per unit area, respectively.

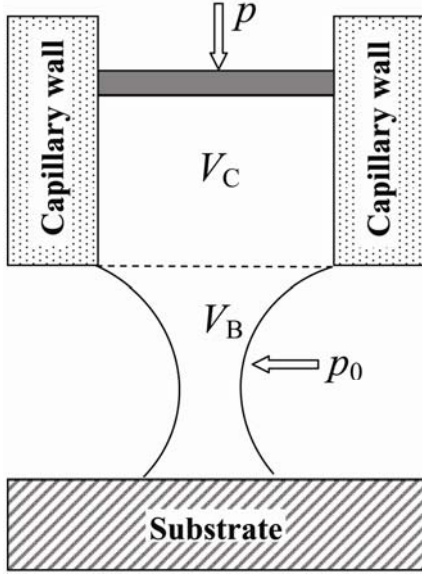


**Figure 1.** Liquid in the bridge (zone  $V_B$ ) and liquid between the (hypothetical) piston and the capillary edge (zone  $V_C$ ) represent a closed system at constant pressure, temperature, and mass (volume).

Using the formulae for  $V_B$ ,  $A_{LV}$ ,  $A_{LS}$  (see Fig. 2 for coordinate system)

$$V_B = \int_0^h \pi r^2(z) dz, \quad A_{LV} = \int_0^h 2\pi r(z) \sqrt{1+r'^2(z)} dz, \quad A_{LS} = \pi r_{BS}^2 \quad (4)$$

where  $r(z)$ ,  $r'(z)$  are the unknown shape function of the liquid bridge and its derivative,  $r_{BS}$  is the unknown radius of the bridge's base on the substrate. Equation (1) for the steady bridge can be presented in the following variational form:

$$\delta F = 0, \quad F = \int_0^h f(r, r') dz - \gamma_{LV} \pi r_{BS}^2 \cos \theta_s^e, \quad (5)$$

$$f(r, r') = 2\pi \gamma_{LV} r(z) \sqrt{1+r'^2(z)} - (p - p_0) \pi r^2(z)$$

where  $\theta_s^e$  is an equilibrium Young-Laplace liquid contact angle on the substrate

$$\cos \theta_s^e = \frac{\gamma_{SV} - \gamma_{LS}}{\gamma_{LV}}. \quad (6)$$

The solution of the variational problem (5) leads to the following necessary equations for the extremum of the functional  $F$  :

$$\frac{\partial f}{\partial r} - \frac{d}{dz} \left( \frac{\partial f}{\partial r'} \right) = 0 \quad (7)$$

$$\left( \frac{\partial f}{\partial r'} \delta r \right) \Big|_{z=0} = 0 \quad (8)$$

$$\left( \frac{\partial f}{\partial r'} - 2\gamma_{LV} \pi r \cos \theta_s^e \right) \Big|_{z=h} \cdot \delta r_{BS} = 0 \quad (9)$$

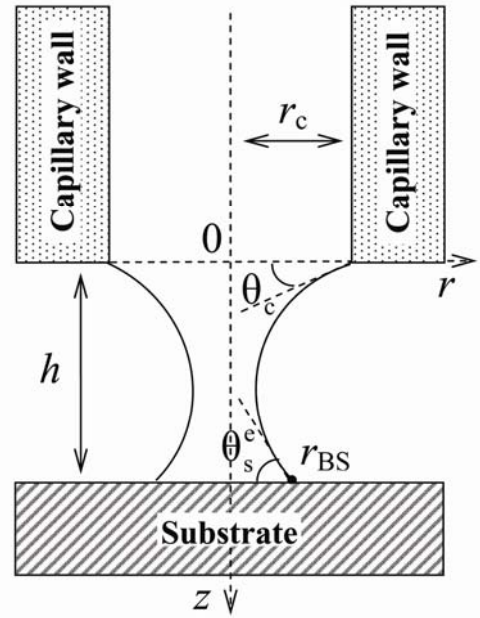


**Figure 2.** Coordinate system used for the modeling of liquid bridge shape between capillary and substrate.

Eq. (7) represents the equation that liquid pressure is uniform inside the bridge and equal to the capillary pressure

$$p - p_0 = \gamma_{LV} \left[ \frac{1}{r \sqrt{1+r'^2}} - \frac{r''}{(1+r'^2)^{3/2}} \right] \quad (10)$$

Equation (8) satisfies the assumption that the top of the liquid bridge is fixed at the inner edge of the capillary

$$r(0) = r_c \quad (11)$$

with the only restriction to the actual contact angle given by

$$\theta_C < \theta_C^e, \quad \cos \theta_C^e = \frac{\gamma_{CV} - \gamma_{LC}}{\gamma_{LV}} \quad (12)$$

where  $\theta_C^e$  is the equilibrium Young-Laplace liquid contact angle on the capillary. Equation (9) can be rewritten as following

$$2\pi\gamma_{LV}(\cos \theta_s - \cos \theta_s^e)r_{BS}\delta r_{BS} = 0 \quad (13)$$

Since the radius of the bridge's base is not fixed, equation (13) is naturally satisfied when the actual liquid contact angle on the substrate is equal to the equilibrium one, calculated from Eq. (6):

$$\theta_s = \theta_s^e \text{ or } r'(h) = -\tan\left(\theta_s^e - \frac{\pi}{2}\right) \quad (14)$$

Thus, the shape of the bridge can be found as the solution of Eq. (10) with boundary conditions (11) and (14).

### 3. EXPERIMENT

The liquid bridge theory presented here was verified in the experiments with glycerol as the deposition liquid ( $\gamma_{LV} = 0.063 \text{ N/m}$ ). A quartz micro-capillary with outer diameter of 1 mm, and inner diameter of  $r_c = 300 \mu\text{m}$  was used in the experiments. The capillary tip was cut with automatic wafer dicing system (ADT Dicing Saw 7500) perpendicular to the capillary axis to get sharp edge. Since the first step of the deposition procedure is the formation of the meniscus protruding out of the capillary, the outer surface of the capillary was made non-wettable to the deposited liquid using the following hydrophobization procedure. Dry capillary was immersed in 0.5 wt. % solution of octadecyltrichlorosilane in toluene for 10 minutes. After that the capillary was rinsed with clean toluene. Using the hydrophobized capillary the menisci with different thicknesses ( $0 < h_M < r_c$ ) could be formed, with the thickness  $h_M$  controlled by applied liquid pressure. Hydrophobized quartz plate was used as a substrate. To evaluate the effectiveness of the hydrophobization procedure the contact angles on a quartz plate (not the capillary) were measured. The glycerol contact angle on the quartz before hydrophobization was equal to  $31^\circ$ ; after hydrophobization it increased to  $95^\circ$ .

The micro-capillary was filled with glycerol. The meniscus was formed due to hydrostatic pressure of the glycerol column. Then the micro-capillary was connected to Newport stages SDS65 in an XYZ assembly and the micro-capillary movement was controlled with micron resolution in all directions. A high speed camera (NanoSense Mk-III, by Dantec Dynamics) was used with magnification lenses to monitor the shape of the formed bridge, the dynamics of bridge rupturing, and the size

of residual droplet. The experimental setup is presented on Fig. 3. The change in capillary/substrate distance was set by software controlling the motion of the stages. The absolute value of the capillary/substrate distance was also checked using photo images of the liquid bridge in which inner diameter of the capillary served as a reference that was measured prior the experiments using optical microscope.

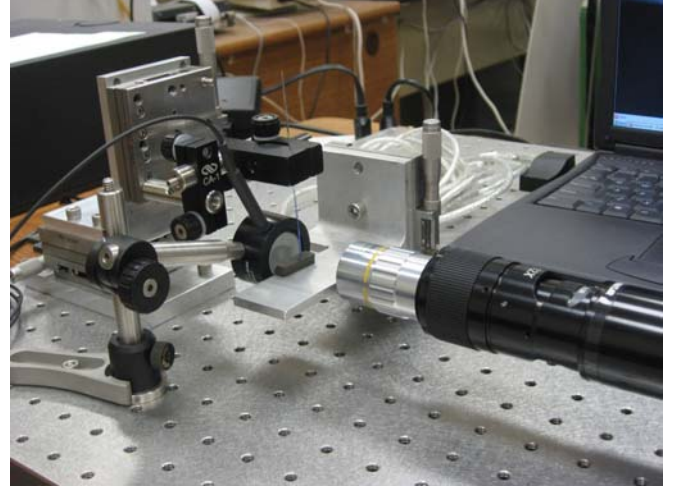


**Figure 3.** Experimental setup used for capillary-based liquid micro deposition.

The deposition scenario is presented in Figs 4 and 5. The normalized distance,  $H = h/r_c$  and the normalized pressure,  $P = (p - p_0)r_c / 2\gamma_{LV}$  are used to characterize the substrate-capillary distance and the liquid pressure respectively. Liquid hydrostatic pressure in the capillary was adjusted such that the liquid meniscus maintained a thickness of  $h_M = 31 \mu\text{m}$  (Fig. 4a). When liquid meniscus just touched the substrate ( $H = 0.20$ ), a liquid bridge formed immediately (Fig. 4b). A steady liquid bridge between capillary and substrate formed after  $\sim 0.3$  sec. (Fig. 4c). The capillary was kept for about 20 minutes at this capillary-substrate distance ( $H = 0.20$ ). Figure 4d shows the shape of this bridge after waiting for about 20 minutes at the capillary-substrate distance of  $H = 0.20$ . No difference between Figure 4c and Figure 4d can be observed. The shape of the stable bridge perfectly agrees with the theoretical predictions shown on Figs 4c and 4d with solid lines. After that the capillary was slowly moving up from the substrate with the retraction velocity of  $3 \mu\text{m/s}$  until the normalized capillary-substrate distance became  $H = 0.40$ . Figure 4e shows the bridge structure at the stopping moment. Figure 4f represents the shape of bridge after waiting about 20 minutes at the capillary-substrate distance of  $H = 0.40$ . Solid lines in Figs 4e and 4f illustrate the calculated shape of the steady bridge for this capillary-substrate distance. Again the stable bridge formed which coincides with the theoretical calculation.

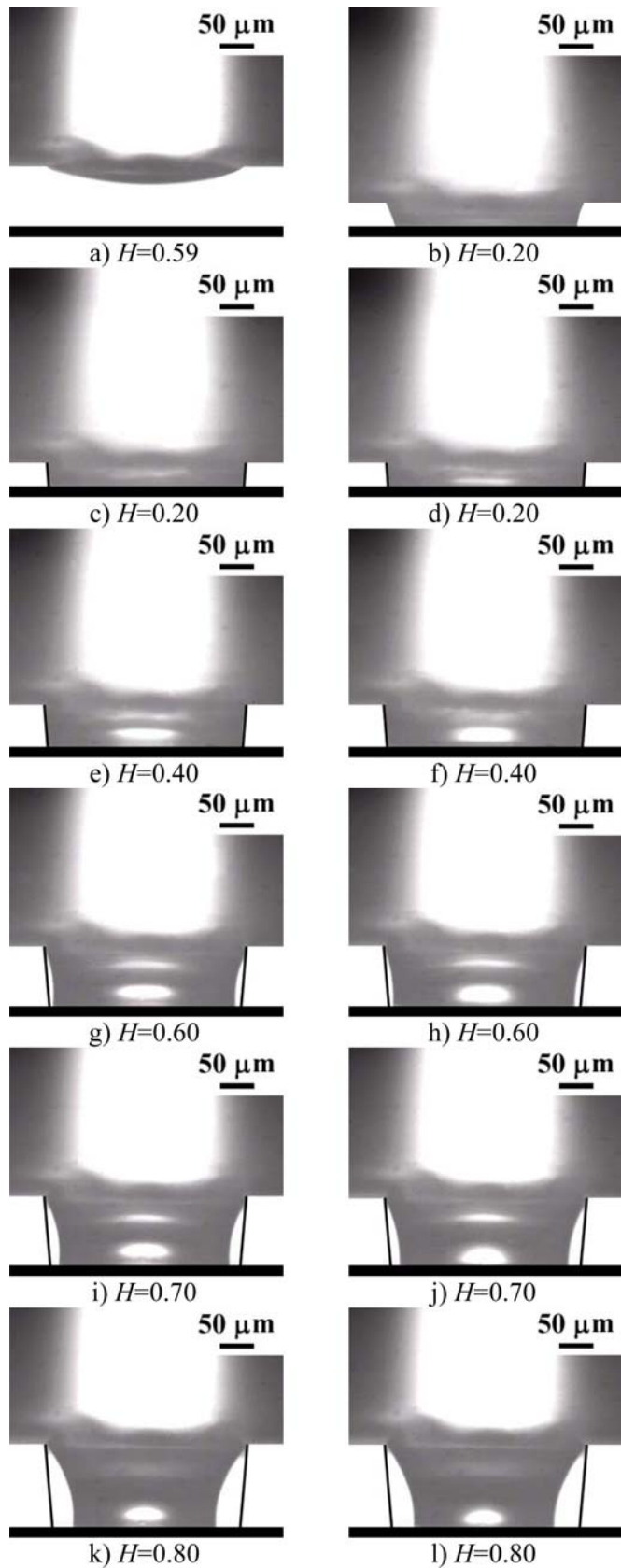


**Figure 4.** First part of deposition scenario for the normalized pressure of  $P = 0.52$ , capillary-substrate distance changes from 0.2 to 0.8. Solid lines in all photos represent the theoretical steady bridge shape.

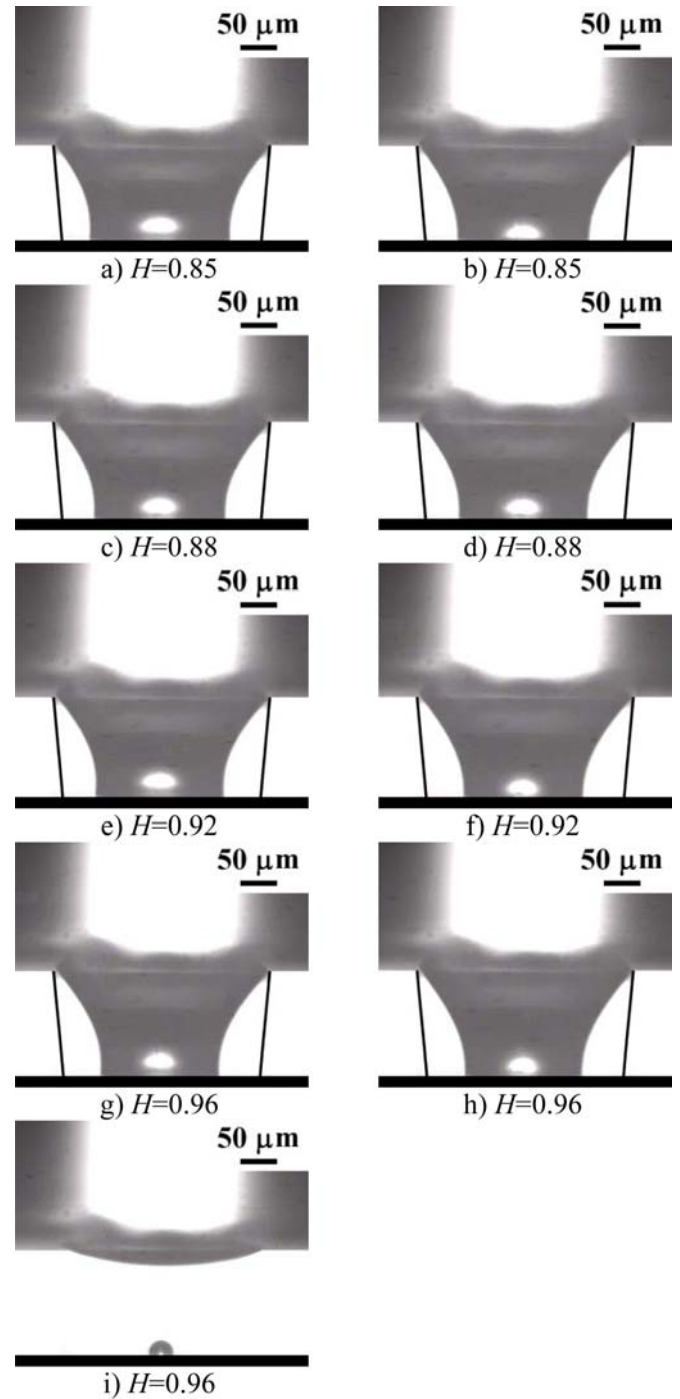


**Figure 5.** Second part of deposition scenario for the pressure of  $P = 0.52$ , capillary-substrate distance changes from 0.85 to 0.96. Solid lines in all photos represent the theoretical steady bridge shape.

Then the capillary was slowly moving up with the velocity of  $3\mu\text{m/s}$  until the normalized capillary-substrate distance became  $H = 0.60$ . Figure 4g shows the bridge structure at the moment of stopping.

It is clear that in spite of very slow retraction velocity the experimental shape of the bridge is still transient and the substrate contact angle is slightly lower than  $\theta_s^e$ . Figure 4h represents the bridge after waiting for about 20 minutes at the capillary-substrate distance of  $H = 0.60$ . We observe that the substrate contact angle increased during the waiting while the base radius remained constant. Solid lines in Figs 4g and 4h illustrate the calculated shape of the steady bridge for this capillary-substrate distance. Note that the experimental bridge shape starts to differ from theoretical calculation.

Again, after waiting the capillary was moving up with the retraction velocity of  $3\mu\text{m/s}$  until  $H = 0.70$ . Figure 4i shows the bridge structure at the moment of stopping and figure 4j represents the bridge after waiting for about 20 minutes at the capillary-substrate distance of  $H = 0.70$ . We found that the substrate contact angle increased during the waiting. At the same time the base radius remained constant. Similar to  $H = 0.60$ , the experimental shape of the bridge does not coincide with theoretical prediction.

And again, after waiting the capillary was moving up with the retraction velocity of  $3\mu\text{m/s}$  until  $H = 0.80$ . Figure 4k shows the bridge structure at the moment of stopping and figure 4l represents the bridge after waiting for about 20 minutes at the capillary-substrate distance of  $H = 0.80$ . The substrate contact angle was found to slightly increase during the waiting. Also the difference between experimental and theoretical bridge shapes is getting more pronounced.

Then the capillary was moving up with the retraction velocity of  $3\mu\text{m/s}$  until  $H = 0.85$ . Figure 5a shows the bridge structure at the moment of stopping and figure 5b represents the bridge after waiting for about 20 minutes at the capillary-substrate distance of  $H = 0.85$ . We found that the substrate contact angle slightly increased during the waiting, but the base radius slightly decreased.

Again the capillary was slowly moving up with the velocity of  $3\mu\text{m/s}$  until the normalized capillary-substrate distance became  $H = 0.88$ . Figure 5c shows the bridge structure at the moment of stopping and figure 5d represents the bridge after waiting for about 20 minutes at the capillary-substrate distance of  $H = 0.88$ . We observe that the substrate contact angle increased during the waiting, and again the base radius slightly decreased.

Then the capillary was moving up with the retraction velocity of  $3\mu\text{m/s}$  until point  $H = 0.92$ . Figure 5e shows the bridge structure at the moment of stopping and figure 5f represents the bridge after waiting for about 20 minutes at the capillary-substrate distance of  $H = 0.92$ . It was found that the substrate contact angle slightly increased during the waiting, and the base radius further decreased.

Again the capillary was slowly moving up with the velocity of  $3\mu\text{m/s}$  until the normalized capillary-substrate distance became  $H = 0.96$ . Figure 5g shows the bridge structure at the moment of stopping and figure 5h represents the bridge after waiting for  $\sim 1$  min at the capillary-substrate distance of  $H = 0.96$ . The substrate contact angle increased during the waiting, and the base radius decreased. Shortly after that the bridge ruptured itself leaving the residual droplet of  $r_d = 17.5\mu\text{m}$  on the substrate (Fig. 5i). The residual droplet radius was defined visually as the radius of the droplet footprint on the substrate. Since substrate contact angle is  $95^\circ$  the actual amount of deposited liquid is approximately half of the mass of a spherical droplet with a radius  $r_d$ .

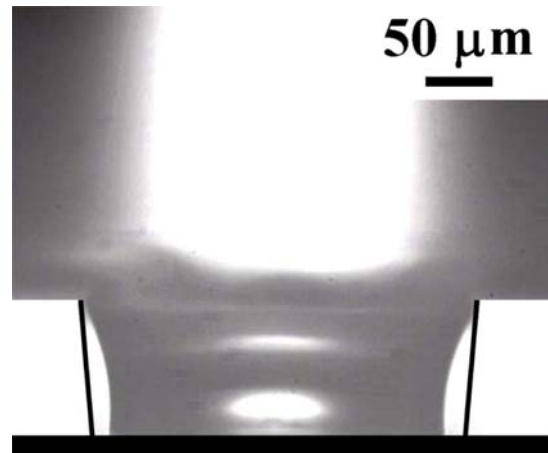


Figure 6. Zoom of Figure 4g.

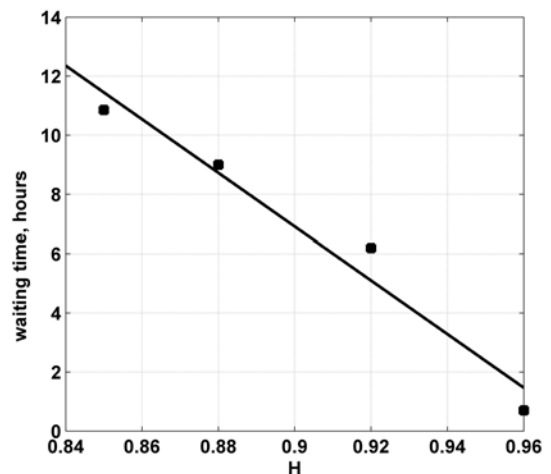


Figure 7. Time needed for bridge rupturing as a function of the capillary-substrate distance.

Thus, for the smaller capillary-substrate distances ( $H < 0.5$ ), the experimental bridge shapes can be predicted from the static theory. At the same time for larger capillary-substrate distances ( $H > 0.5$ ), the experimental bridge shapes cannot be described

by static theories even for such a low velocity of retraction as 3  $\mu\text{m/s}$ . In order to fully capture the experimental phenomena, the dynamics of the bridge has to be taken into consideration.

Due to retraction, the bridge substrate contact angle is getting lower than the equilibrium contact angle. This is shown in Fig. 6 which is a magnification of Fig. 4g. After the waiting period, the bridge substrate contact angle tends to increase to liquid droplet equilibrium contact angle, but the time needed for the process is very long and is dependent on the capillary-substrate distance. While the capillary-substrate distance  $H$  is lower than 0.8, the base radius has a tendency to stay constant when retraction is stopped and  $H$  is held constant. But as soon as the capillary-substrate distance is higher than 0.8, the base radius decreases. Based on the experimentally measured rate of change for the base radius, the waiting time needed for the bridge rupturing can be roughly extrapolated. Figure 7 shows the dependency between the capillary-substrate distance and the time needed for the bridge rupturing.

#### 4. CONCLUSIONS

A capillary-based lithography method is described where the substrate is untouched by the dispensing tip. The application of the pressure from one side of capillary causes the liquid meniscus to form at the capillary outlet. Touching the substrate with the liquid meniscus causes the liquid deposition on the substrate. Deposition of glycerol as a trial liquid was realized on the micro-scale. The size of deposited liquid droplet is about 10% of inner diameter of the capillary. Comparison of theoretical results with experimental data shows good agreement for  $H < 0.5$ . A detailed theoretical/experimental study of the problem for a wide range of contact angles  $\theta_c^e$ ,  $\theta_s^e$  and capillary radii  $r_c$  will be presented in Ref. [5]. As the next step, it is planned to scale this method down to nanoscale using nanocapillary navigated by Scanning Tunneling Microscope.

#### ACKNOWLEDGEMENTS

This work is supported by North Dakota EPSCoR and National Science Foundation Grant EPS-0814442.

#### REFERENCES

- [1] R.D. Piner, J. Zhu, F. Xu, S.H. Hong, and C.A. Mirkin, Dip Pen Nanolithography, *Science*, vol. 283, pp. 661-663, 1999.
- [2] S. Deladi, N.R. Tas, J.W. Berenschot, G.J.M. Krijnen, M.J. de Boer, J.H. de Boer, M. Peter, and M.C. Elwenspoek, Micromachined fountain pen for atomic force microscope-based nanopatterning, *Applied Physics Letters*, vol. 85, no. 22, pp. 5361-5363.
- [3] A. Meister, M.Liley, J. Brugger, R. Pugin, and H. Heinzelmann, Nanodispenser for attoliter volume deposition using atomic force microscopy probes modified by focused-ion-beam milling, *Applied Physics Letters*, vol. 85, no. 25, pp. 6260-6262.
- [4] B. Qian, M. Loureiro, D.A. Gagnon, A. Tripathi, and K.S. Breuer, Micron-Scale Droplet Deposition on a Hydrophobic Surface Using a Retreating Syringe, *Physical Review Letters*, vol. 102, 164502, 2009.
- [5] A. Lutfurakhmanov, G.K. Loken, Y. Wang, D.L. Schulz, and I.S. Akhatov (manuscript in preparation).